



Article

Transcriptomic and Metabolomic Analysis Reveal Possible Molecular Mechanisms Regulating Tea Plant Growth Elicited by Chitosan Oligosaccharide

Dezhong Ji ¹, Lina Ou ¹, Xiaoli Ren ¹, Xiuju Yang ^{1,2}, Yanni Tan ¹, Xia Zhou ^{1,*} and Linhong Jin ^{1,*} 

- ¹ State Key Laboratory Breeding Base of Green Pesticide and Agricultural Bioengineering, Key Laboratory of Green Pesticide and Agricultural Bioengineering, Ministry of Education, Guizhou University, Guiyang 550025, China; gs.dzji19@gzu.edu.cn (D.J.); gs.lnou17@gzu.edu.cn (L.O.); gs.xlren20@gzu.edu.cn (X.R.); gs.xjyang20@gzu.edu.cn (X.Y.); gs.yntan20@gzu.edu.cn (Y.T.)
- ² College of Tea, Guizhou University, Guiyang 550025, China
- * Correspondence: xzhou@gzu.edu.cn (X.Z.); lhjin@gzu.edu.cn (L.J.); Tel.: +86-851-3620-521 (X.Z. & L.J.)

Abstract: Chitosan oligosaccharide (COS) plays an important role in the growth and development of tea plants. However, responses in tea plants triggered by COS have not been thoroughly investigated. In this study, we integrated transcriptomics and metabolomics analysis to understand the mechanisms of chitosan-induced tea quality improvement and growth promotion. The combined analysis revealed an obvious link between the flourishing development of the tea plant and the presence of COS. It obviously regulated the growth and development of the tea and the metabolomic process. The chlorophyll, soluble sugar, and amino acid content in the tea leaves was increased. The phytohormones, carbohydrates, and amino acid levels were zoomed-in in both transcript and metabolomics analyses compared to the control. The expression of the genes related to phytohormones transduction, carbon fixation, and amino acid metabolism during the growth and development of tea plants were significantly upregulated. Our findings indicated that alerted transcriptomic and metabolic responses occurring with the application of COS could cause efficiency in substrates in pivotal pathways and hence, elicited plant growth.

Keywords: chitosan oligosaccharide; tea plant growth and development; transcriptome; metabolic pathways; metabolism



Citation: Ji, D.; Ou, L.; Ren, X.; Yang, X.; Tan, Y.; Zhou, X.; Jin, L. Transcriptomic and Metabolomic Analysis Reveal Possible Molecular Mechanisms Regulating Tea Plant Growth Elicited by Chitosan Oligosaccharide. *Int. J. Mol. Sci.* **2022**, *23*, 5469. <https://doi.org/10.3390/ijms23105469>

Academic Editor: Bartolomé Sabater

Received: 7 April 2022

Accepted: 11 May 2022

Published: 13 May 2022

Publisher's Note: MDPI stays neutral with regard to jurisdictional claims in published maps and institutional affiliations.



Copyright: © 2022 by the authors. Licensee MDPI, Basel, Switzerland. This article is an open access article distributed under the terms and conditions of the Creative Commons Attribution (CC BY) license (<https://creativecommons.org/licenses/by/4.0/>).

1. Introduction

The quantity and quality of tea leaves are mainly affected by the metabolites in tea leaves, such as tea polyphenols, theanine, caffeine, vitamins, volatile oils, polysaccharides, and minerals, which are closely related to the growth process of tea trees [1]. Tea plant pests and diseases and environmental pressure cause major economic losses for tea. Traditional pesticides can increase the yield of tea, but their residues would be harmful to the local ecosystem and the quality of the tea plant [2–6]. The application of natural-origin chitosan has been reported safe for the environment and beneficial to the quality and yield of crops [7–10].

Chitosan oligosaccharides (COS) are derived from the shells of shrimp and other sea crustaceans and possess good water solubility and a wide range of biological activity [11]. Chitosan has generated great attention in a range of fields due to its exceptional biological activities, especially in agricultural uses like antimicrobial action [12,13], plant growth and development promotion [14–16], plant defenses elicitation [13], and resistance against various abiotic stresses [12,14,17]. For example, it augments plant height, leaf number, fruit weight, number, and yield [18–20]. Chitosan can improve the growth shoot and root length in beans [21]. The promotion function of chitosan application is also verified in several other plants, such as potatoes [22], wheat [23], and rice [24]. Chitosan can increase

chlorophyll content and thus photosynthesis in rape seedlings [25] or up-regulate a series of primary C and N metabolic pathways in the leaves of wheat seedlings [26]. We have previously reported that chitosan has obvious promoting effects on tea plant growth [27] and eliminates the cold stress on the tea plant [28]. This biodegradable, economical, and renewable oligosaccharide is more appealing in organic agriculture and benefits plant yields and ecological biodiversity.

Most previous studies have been limited to the apparent effects of chitosan on plant physiology and growth characteristics. However, no research has confirmed the metabolic responses of chitosan on tea plant growth and the yield promotion of chitosan in the tea tree. At the same time, plant histological techniques are widely used for the discovery of functional genes, identification of metabolic pathways, and modification of plant cell characteristics [29–31]. Metabolite profiling technology is critical to the comprehensive analysis of the plant growth mechanism [32–34]. Multiparametric metabolic response of plants can be achieved by metabolomics, where metabolic accumulation and change could be detected by chromatography interfaced with mass spectrometry [32].

However, despite the elicitors function of chitosan discovered to date, alterations or responses in tea plants triggered by it have not been thoroughly investigated. Therefore, biochemical analysis of the tea plant by integrating transcriptomics and metabolomics analysis will aid our understanding of the mechanisms of chitosan-induced tea quality improvement and growth-promoting.

In this study, we compared metabolic profiles of control and chitosan-treated leaves and relationships within the metabolic network of the tea plant. Using this approach, we determined that a chitosan-induced metabolic strategy can increase the normal regulation of amino and nucleotide sugar metabolism, which enables intrinsic growth promotion.

2. Results

2.1. Yield Measurement of Tea Leaves

The data of tea yield, including bud density, were measured as shown in Table 1. The concentration of COS at 2.0 g/667 m² (1:800) performed better but with no significant difference. The average bud densities were 122.3, 128.8, and 126.9 buds for the three concentrations 1.6, 2.0, and 3.2 g/mu (1 mu = 667 m²), which increased by 18.97, 25.29, and 23.44% when compared to CK. Accordingly, the mean 100-bud weight was 7.68, 7.77, and 7.70 g and increased by 13.66, 15.06, and 14.03% compared to CK. Actual tea leave yield was 33.96, 36.33, and 34.66 g/m² and increased by 15.7, 23.8, and 18.1%, respectively. In sum, the presence of COS can significantly increase the tea plant yield. In contrast, the concentration of COS at 2 g/667 m² performed better, though with no significant difference.

Table 1. Tea yield compared between CK and COS treatment in field test.

| Yield Indicators | CK | COS Treatment (with Different Times of Dilution) | | |
|-----------------------------------|---------------|--|-------------------------------------|--------------------------------------|
| | | 3.2 g/667 m ² (1:500) | 2.0 g/667 m ² (1:800) | 1.6 g/667 m ² (1:1000) |
| Bud density (bud/m ²) | 1028 ± 48b | 1223 ± 60a | 1288 ± 38a | 1269 ± 64a |
| 100-bud weight (g/100 bud) | 6.76 ± 0.04b | 7.68 ± 0.07a | 7.77 ± 0.04a | 7.70 ± 0.07a |
| Actual output (g/m ²) | 29.35 ± 0.10b | 33.96 ± 0.04a | 36.33 ± 0.06a | 34.66 ± 0.08a |

The value represents the mean ± SD of three biological repeats. Different letters indicate significant differences at $p < 0.05$.

Among the three tested concentrations, 800-time dilution performed best. Both the higher and lower concentrations spoiled the effect rather than increasing the production yield. Therefore, we applied and checked the most effective 800-time for their function.

As shown in Figure 1, more fresh shoots from the tea bushes were exposed in the COS treatment than in that of the control group. In addition, the promoted emergence of new and tender leaves could be compared by bud density and 100-bud weight.



Figure 1. Tea plants bearing fresh tea shoots seven days after treatment (left: COS-treated tea plant at the concentration of 2.0 g/667 m²; right: CK).

2.2. Changes of Chlorophyll, Soluble Sugar, and Amino Acid Content in Tea Leaves

The effects of COS treatment on the contents of the total amino acids, chlorophyll, and soluble sugar in the tea leaves were investigated. The values for those tested parameters in the COS group were obviously higher than in the control group (Figure 2A). Among them, the amino acids in the COS-treatment group were 60.77 mg/g FW and 39.86% higher than in the CK group (43.45 mg/g FW). Similarly, the chlorophyll content in the COS treatment was 0.41 mg/g FW and 64% higher than in the control (0.18 mg/g FW), with great significance (Figure 2B). In addition, the soluble sugar content of COS treatment was 83.37 mg/g FW and increased by 17.76% compared to the control group (Figure 2C).

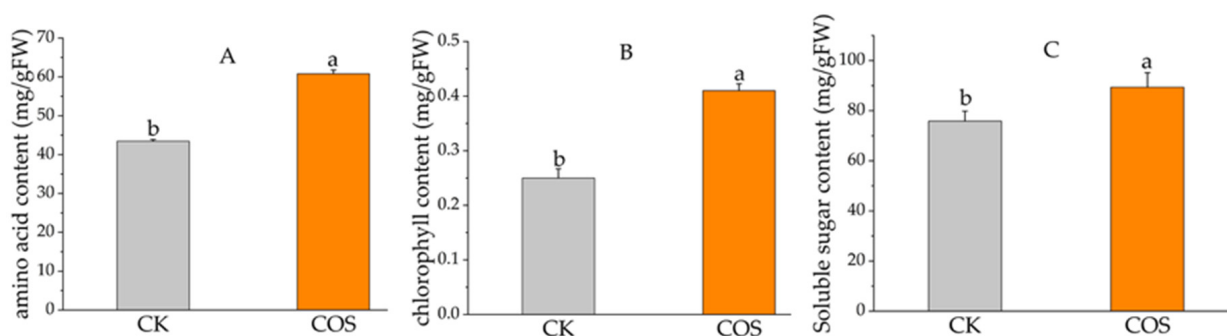


Figure 2. Effects of COS on amino acid, chlorophyll, and soluble sugar content. (A) Amino acid content; (B) Chlorophyll content; (C) Soluble sugar content. The value of the vertical axis represents the mean \pm SD of three biological repeats. Different letters indicate significant differences at $p < 0.05$.

2.3. Transcriptomic Analysis

2.3.1. Transcriptome Sequencing and Assembly

In this study, both COS and CK group samples were sequenced by the Illumina Nova seq platform. A total of 70–106 million raw reads were obtained for the COS group three repeats and 76 to 96 million raw reads for the CK group, respectively. After filtering, 66.2–100.0 million clean reads were obtained for the COS group and 70–90 million reads for the control. In all groups, Q20 was 100%, Q30 was above 99%, and the average GC contents of the CK group and COS group were also above 46%. The results indicated that the sequencing is of high quality and could be used for further analysis (Table 2).

Table 2. Throughput and quality summary of RNA-sequence.

| Samples | Raw Reads | Clean Reads | Q20 (%) | Q30 (%) | GC (%) |
|--------------|-----------|-------------|---------|---------|--------|
| TreT7_1(COS) | 84011624 | 78935806 | 100 | 99.4 | 46.81 |
| TreT7_2(COS) | 106371756 | 99995940 | 100 | 99.3 | 46.73 |
| TreT7_3(COS) | 70432706 | 66250686 | 100 | 99.3 | 46.73 |
| ConT7_1(CK) | 81114666 | 75623100 | 100 | 99.3 | 46.94 |
| ConT7_2(CK) | 96205136 | 89960092 | 100 | 99.3 | 46.74 |
| ConT7_3(CK) | 76155870 | 70900816 | 100 | 99.3 | 46.8 |

2.3.2. Differentially Expressed Gene (DEG) Analysis

The biological repeatability between samples was analyzed using Spearman analysis to verify the high correlation of gene expression levels between samples and proved that a perfect Spearman correlation occurred based on the RPKM (Reads per Kilobase per Million) of different samples. Genes with p -value < 0.05 and $|\log_2(\text{Fold Change})| > 1$ were defined as DEGs (genes that were differentially expressed between control and COS). A total of 5806 DEGs were identified between two groups of tea leave samples, of which 3262 up-regulated genes and 2544 down-regulated genes were found (Table S1).

2.3.3. Gene Ontology (GO) Annotation

Gene ontology (GO) provides the representation of gene product attributes and covers three domains: cellular component (CC), molecular function (MF), and biological process (BP). The GO annotation for the two groups revealed that a major part of DEGs was involved in BP, and MF covered DEGs with high rich factors (Figure 3 and Table S2). The main CC categories (the parts of a cell or its extracellular environment) were “intracellular organelles” (GO:0043229), “cytoplasm” (GO:0005737), and “organelles part” (GO:0044422), and so on. The main MF category (the elemental activities of a gene product at the molecular level) was the expression of genes related to transferase activity at the molecular level, such as “methyltransferase activity” (GO:0008168), “transferase activity” (GO:0008168), “serine hydrolase activity” (GO:0017171), and “ubiquitin-protein transferase activity”(GO:0004842). In terms of BP, the main categories focus on metabolic processes or molecular events, such as the “protein metabolic process” (GO:0019538), the phosphorus metabolic process (GO:0006793), and the cellular amino acid metabolic process (GO:0006520).

2.3.4. Kyoto Encyclopedia of Genes and Genomes (KEGG) Annotation

The degree of enrichment of KEGG was measured by the abundance factor, p -value, and the number of genes in the pathway. The significance of enrichment is shown on the horizontal coordinates; the greater the value ($-\log_{10}(p\text{-value})$), the more significant the enrichment. The KEGG pathway is shown on the longitudinal coordinates in Figure 4. The size of the dots indicates the number of different genes contained in the KEGG pathway, and the color of the dots indicates the degree of rich factor enrichment. These enriched pathways include “starch and sucrose metabolism” (ko00500), “glycolysis/gluconeogenesis” (ko00010), “biosynthesis of amino acids” (ko01230), “plant hormone signaling” (ko04075) (Figure 4, Table S3). The DEGs were significantly enriched in pathways for “starch and

sucrose metabolism”, “phytohormone signal transduction”, “Phenylpropanoid biosynthesis”, “glycolysis/gluconeogenesis”, “glycerophospholipid metabolism”, “fatty acid metabolism”, “cysteine and methionine metabolism”, “the carbon fixation of photosynthetic organisms”, “the biosynthesis of amino acids”, “the biosynthesis of unsaturated fatty acids”, and other genes closely related to plant growth and development, which were all significantly up-regulated.

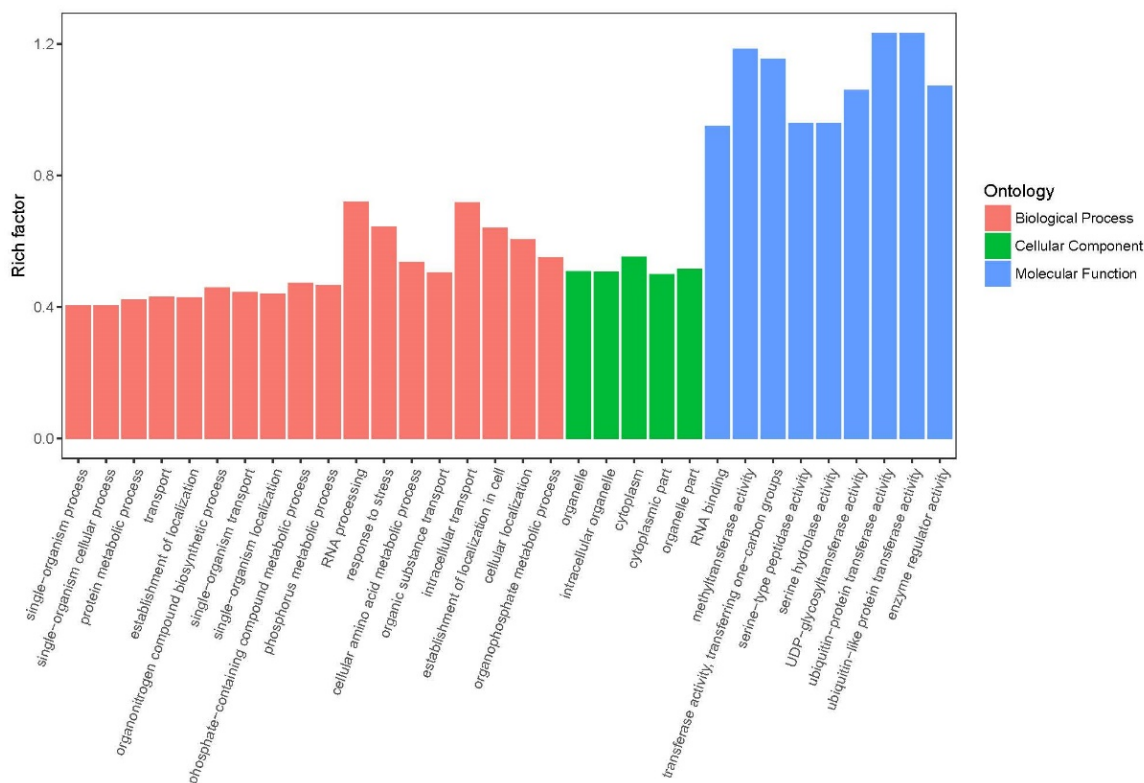


Figure 3. GO classification analysis based on DEGs.

The differentially expressed genes (DEGs) involved in response to COS were summed up and analyzed. Many DEGs are found related to pathways related to the growth and development of tea plants, including plant hormone signal transduction, starch, and sucrose metabolism, phenylpropanoid biosynthesis, glycolysis/gluconeogenesis, and carbon fixation in photosynthetic organizations, and biosynthesis of amino acids. The DEGs involved in the main metabolic pathways, including plant hormone signal transduction, carbohydrate metabolism, photosynthesis, amino acid metabolism, and other physiological and biochemical processes related to tea growth and development, are displayed in Tables S4–S9. These DEGs were characterized as genes encoding auxin-responsive GH3 gene family (GH3), SAUR family protein (SAUR), auxin influx carrier (AUX1), histidine-containing phosphotransfer protein (AHP), alpha-amylase (AMY), sucrose synthase (SUS), fructose-1,6-bisphosphatase I (FBP), trehalose-phosphatase (otsB), sucrose phosphate synthase (SPS), sucrose synthase (SS), malate dehydrogenase (MDH), carbonic anhydrase (CA), glutamine synthetase (GLUL), glutamate dehydrogenase (GDH), tryptophan (trpB) synthase and so on. Among them, glutamine synthetase (GLUL) and tryptophan (trpB) synthase are DEGs specifically belonging to tea in biosynthesis amino acids.

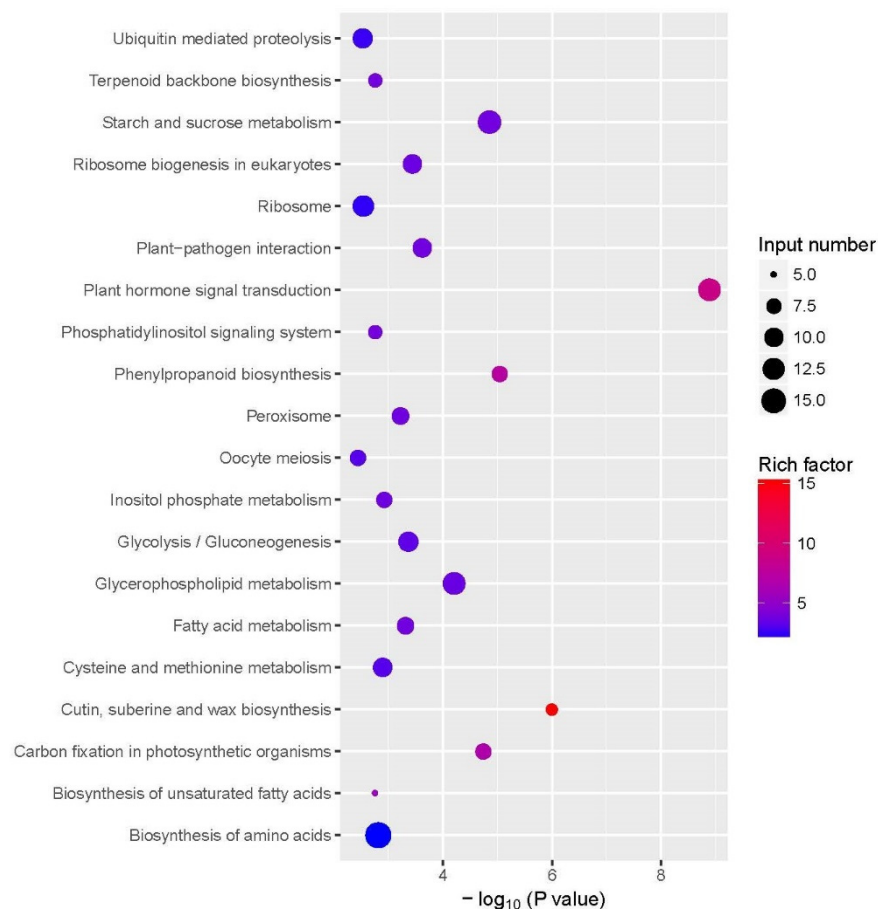


Figure 4. KEGG enrichment analysis of upregulated DEGs response to COS treatment.

2.3.5. Validation of qRT-PCR (Quantitative Real-Time Polymerase Chain Reaction)

To validate the accuracy and repeatability of the transcriptome analysis, qRT-PCR (Figure 5) was performed on a set of DEGs selected randomly from the above acquired DEGs. Results showed that the qRT-PCR expression profiles were consistent with their abundance changes identified by RNA-seq (Table S1), which verified the reproducibility and credibility of RNA-seq data. Results confirmed that AMY, SUS, SAUR, and GH3 were significantly upregulated by exogenous COS.

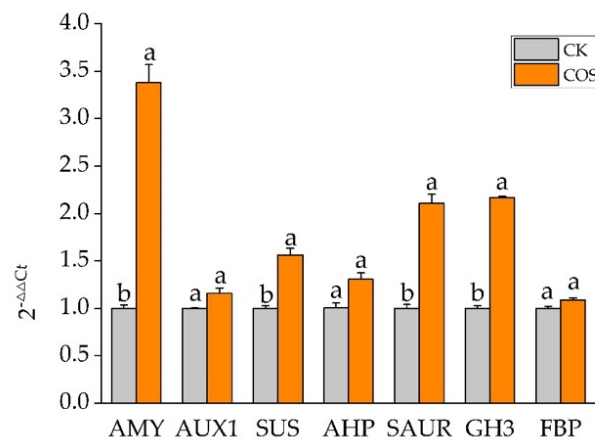


Figure 5. qRT-PCR analysis on randomly selected DEGs.

2.4. Metabolome Data Analysis

2.4.1. Effect of COS on Differential Changes in Tea Metabolites

To examine metabolite patterns elicited by COS, metabolites were extracted from the leaves of the control and COS groups, followed by detection, respectively. Metabolomic analysis of the tea samples by UPLC-QTOF MS in positive mode (ESI⁺) and negative mode (ESI⁻) mode detected. Principal components analysis (PCA) score plots ($n = 6$ for each control and COS-treated sample from tea plant)) revealed discriminative metabolic levels between the tea plant sample of COS and the control group in both pos and neg-modes (Figure 6). The score scatter plots classified samples as COS treatment “HAI7_2” and control “KB7_1”, with 47.57 and 55.91% of the variability contained in PC1 in positive and negative mode, respectively.

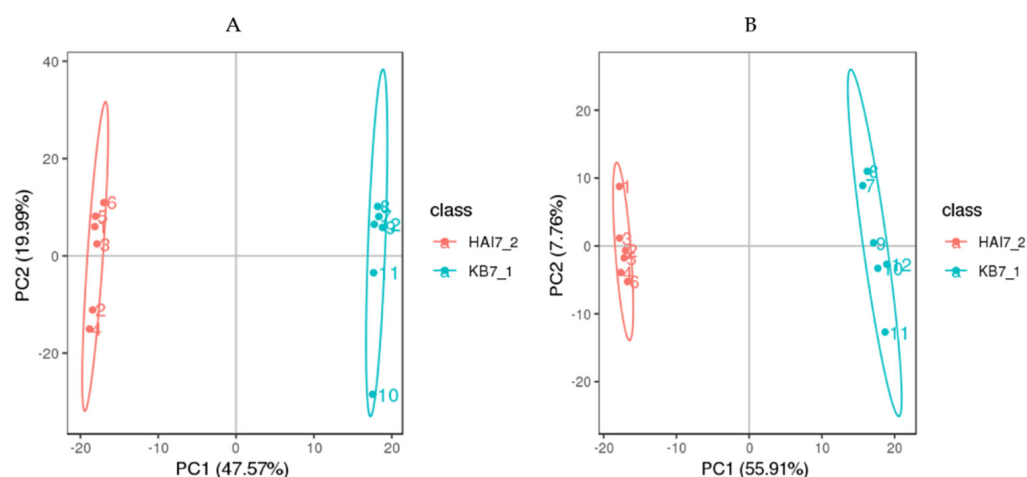


Figure 6. Principal components analysis (PCA) of metabolites. (A) is the positive ion mode, and (B) is the negative ion mode. Red represents the samples of COS treatment (HAI7_2), and the green represents control (KB7_1).

By setting the threshold for significantly differential metabolites (DMs) screening at variable importance in the projection (VIP) > 1.0, $p < 0.05$, a total of 416 DMs were obtained. The content of each metabolite was leveled to complete hierarchical linkage clustering as presented in the heatmap. Each sample was visualized in a single column (COS treatment sample: H7_2_1-H7_2_6; control: K7_1_1-K7_1_6), and each metabolite is represented by a single row [Figure 7, Table S4]. Of which 108 DMs were significantly upregulated and 116 DMs were significantly downregulated in positive mode, 90 were upregulated, and 112 were downregulated in negative mode (Table 3).

Table 3. Metabolites test results.

| Compared Samples | Total Metabolites | Total DMs | Upregulated DMs | Down Regulated DMs |
|---------------------|-------------------|-----------|-----------------|--------------------|
| COS vs. control pos | 748 | 224 | 108 | 116 |
| COS vs. control neg | 591 | 192 | 90 | 102 |

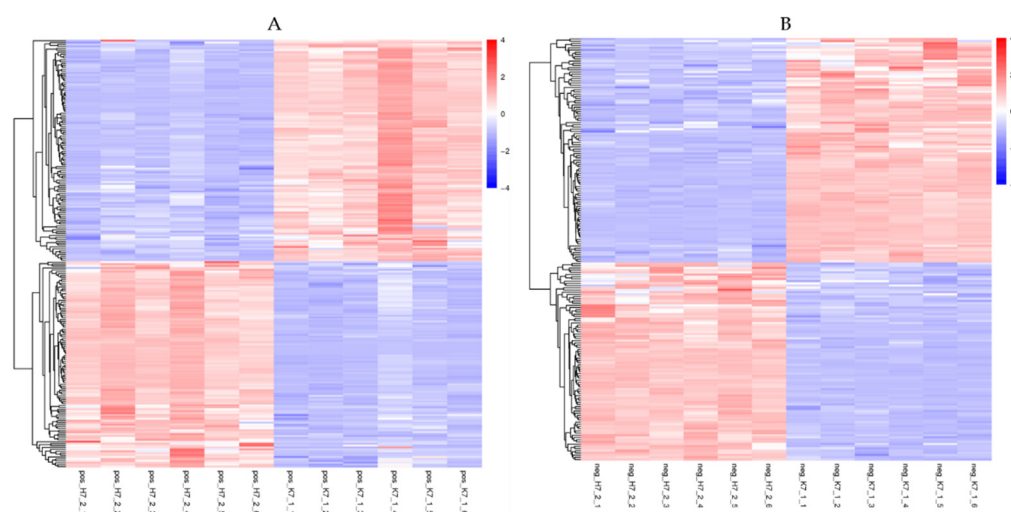


Figure 7. Heatmap of metabolites. Red indicates high abundance, whereas low relative metabolites are shown in blue ((A): positive ion mode, (B): negative ion mode). COS treatment sample: H7_2_1-H7_2_6; control: K7_1_1-K7_1_6).

2.4.2. KEGG Analysis of DMs Response to COS Treatment

KEGG pathways were organized and analyzed to explore the functions of COS on the DMs related to tea plant development (Figure 8). The color of the point represents the p -value of the hypergeometric test. The smaller the value, the more reliable and statistically significant the result is. The size of the dots represents the number of differential metabolites in the corresponding pathway; the larger size indicates a higher significant differential of metabolites in the pathway. It could be seen that the DMs were mainly enriched in the following six pathways, “biosynthesis of secondary metabolites”, “Phenylpropanoid biosynthesis”, “flavone and flavonol biosynthesis”, “alpha-Linolenic acid metabolism”, “Biosynthesis of unsaturated fatty acids”, “Arachidonic acid metabolism”, and “Glutathione metabolism” (Figure 8, Table S10). DMs enriched in these metabolic pathways may play an immediate physiological role and promote and influence growth and development. Among them, the most enrichment of differential metabolites pathway is the biosynthesis of secondary metabolites, and 33 DMs were found in it (Table S11), including amino acids (L-Histidine, L-Ornithine, L-Asparagine), organic acids (Loganic acid, Ferulic acid, Ascorbic acid), flavonoids (Rutin, Kaempferol, Quercetin), and other compounds. The above results showed that COS treatment could significantly increase the production of secondary metabolites in tea plants, thereby promoting the growth and development of tea plants.

2.5. Combination of the Metabolic Profiling and Transcriptomic Analysis

The transcriptomic analysis showed that DEGs in pathways of the plant hormone signal transduction, starch, and sucrose metabolism, phenylpropanoid biosynthesis, glycolysis/gluconeogenesis, and carbon fixation in photosynthetic organizations, and biosynthesis of amino acids of tea plants were significantly enriched in COS treatment. Metabolomics data indicated a total of 1339 differential metabolites were enriched in different metabolic pathways, including the most enriched biosynthesis of secondary metabolites and phenylpropanoid biosynthesis. A combined metabolic and transcriptomic analysis was performed to investigate the potential for the regulation of related metabolites. The result showed that the DEGs and DMs were significantly up-regulated in phenylpropane metabolism pathways. It may refer that the differential genes and metabolites in phenylpropane metabolism play an important role in the growth and development of tea plants. The DEGs and DMs in the phenylpropanoid biosynthesis pathway were summarized and sorted through the KEGG database (Table S12). The metabolic intermediates and end products of the

phenylpropanoid biosynthesis pathway were mapped to the known KEGG pathway. The overall trends of the phenylpropanoid biosynthesis pathway suggested an increase both in metabolic intermediates (such as ferulic acid and coniferyl-aldehyde) and end products (such as coniferin and sinapyl alcohol) by spraying COS on tea plants (Figure 9).

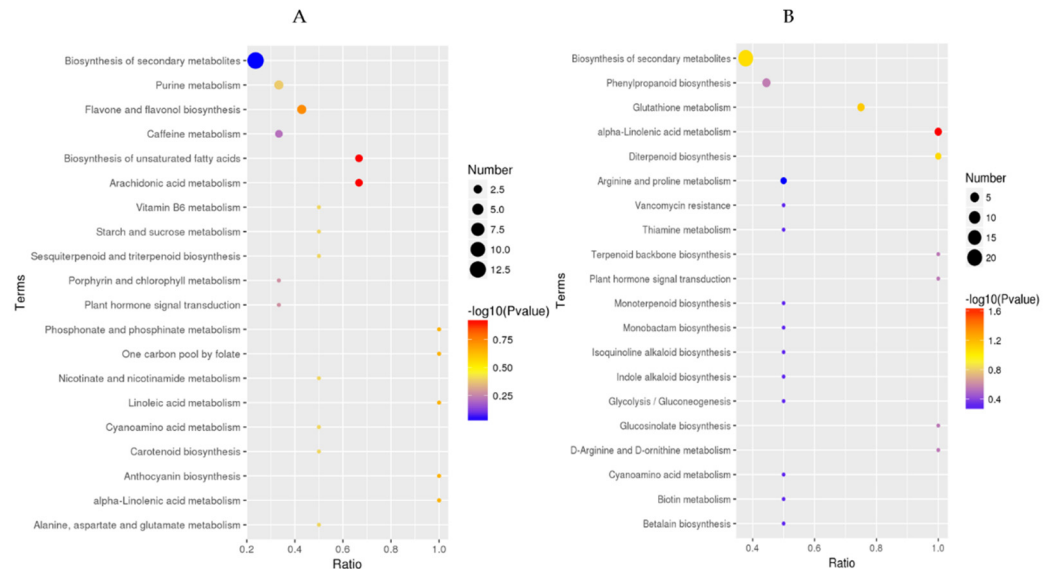


Figure 8. KEGG analysis at positive ion mode (A) and negative ion mode (B). The abscissa is x/y (x: number of differential metabolites in the corresponding metabolic pathway, y: total metabolites identified in this pathway). The higher the value, the higher the enrichment of differential metabolites in this pathway.

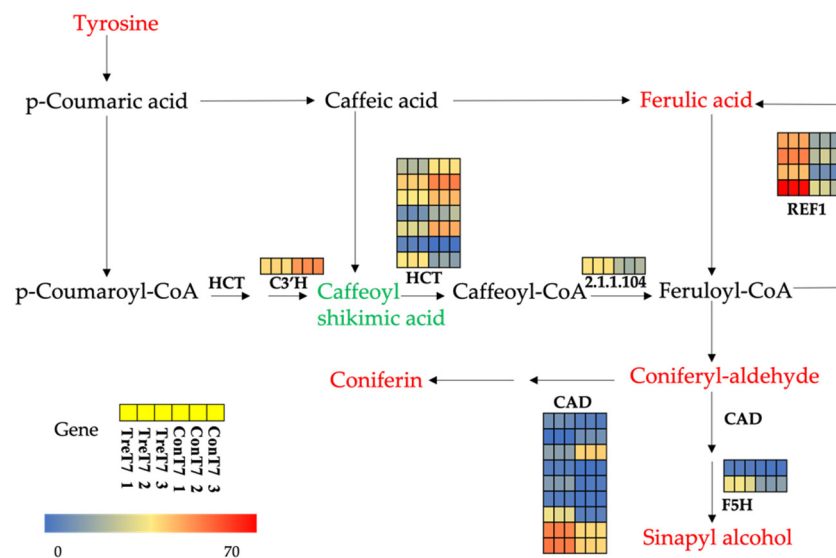


Figure 9. Schematic of a portion of phenylpropanoid biosynthesis pathway in tea plant. Among them, the differential metabolites are marked in red and green, red means up-regulated, and green means down-regulated. Differentially expressed genes are marked next to related enzymes in the form of a heat map. The gene scale bar corresponds to the range of relative transcriptional levels of enzymes.

3. Discussion

In the past few decades, numerous studies have confirmed that chitosan oligosaccharides play an important role in promoting plant growth and development [16,21–23] and plant defense elicitation [13] in various crops. This present study was designed to provide more information and expand the understanding of how this elicitor COS works on tea

plants, as in research [27,28] we have focused on in the past few years. We explored the function of COS on tea plants by integrating analysis of transcriptomics and metabolomics besides the yield indexes and some physiological parameters. The bud density, 100-bud-weight, and actual yield in the COS treatment group were significantly higher than those of the control group. The contents of total amino acids, chlorophyll, and soluble sugar in the tea plant were ascertainably improved by 17.76%, 39.86%, and 64%, respectively. The actual yield (biomass) of tea was increased by 23.8%. These results concluded that COS could indubitably and significantly promote tea plant growth and yield. The chlorophyll content was remarkably increased in the COS-treated tea plant. It extensively corroborated the previous reports on tea plants [27] and other crops [16,17,35].

The chlorophyll content is an important index to measure the rate of plant photosynthesis [36]. COS could improve the content of photosynthetic pigments in various plants [37,38]. COS could induce the synthesis of phytohormones, such as gibberellins and auxin, to enhance growth and development [39] and enhance endogenous concentration [40]. Our present RNA sequencing indicated that COS activated some important metabolic activities and cell processes in tea plants. In addition, they significantly changed the expression level of genes involved in plant hormone signal transduction, photosynthesis, carbon metabolism, and amino acid metabolism. AUX1, GH3, and SAUR are the important genes encoding auxin, and the AHP gene which encodes cytokinin. Additionally, the DELLA protein (DELLA) and phytochrome interacting factor 3 (PIF3) encoding gibberellin were significantly upregulated. The above results show that spraying COS on tea plants can regulate plant growth by regulating the expression of genes related to plant hormones.

The synthesis of carbon compounds (activated by carbonic anhydrase) is directly related to photosynthesis and the growth and development of plants [41]. In the present research, COS upregulated photosynthetic organisms, starch and sucrose metabolism, and Glycolysis/Gluconeogenesis, as important components of plant carbon metabolism, played an important role in plant growth and development. The overexpressing of cytosolic FBP and SPS both resulted in the accumulation of sucrose, as reported [42,43]. Sucrose synthase (SUS) is a class of enzymes that are widely considered to be the main pathway for sucrose carbon to enter plant cell metabolism and play a key role in plant development. In our research, the chlorophyll content in the COS treatment group was increased and the genes encoding CA, FBP, SPS, and SUS were also significantly upregulated (Table S9). The above results indicated that COS application on tea plants could enhance the photosynthetic CO₂ fixation and the accumulation of photosynthetic assimilates, which as an endogenous correlation, further contributes to the improvement of the photosynthesis and growth of tea plants. Similarly, the content of soluble sugar in the COS treatment group was significantly higher than that in the control group.

Apart from the enhanced photosynthesis, the key genes involved in carbon and nitrogen metabolism were also upregulated by COS. It has been well-documented that carbon and nitrogen are both primary nutrients for plant growth and crop yields [44]. In the present study, genes encoding trehalose-phosphatase, PEPC, MDH, and glutamate dehydrogenase were significantly upregulated (Table S9), which was consistent with the results obtained in rice plants [45]. Studies have proved that the net accumulation of organic acids could act as a C-skeleton for the synthesis of amino acids in nitrogen assimilation [46]. In our study, amino acid metabolism was significantly activated, and key enzymes in related metabolic pathways were significantly upregulated, such as GLUL, trpB, GS, and GDH. Metabolomics data also showed up-regulated expression of amino acid compounds, such as L-Tyrosine, L-Histidine, L-Asparagine, and L-Ornithine (Table S4). The amount of total amino acids extracted from the tea leaves increased correspondingly in the COS-treated group. DEGs upregulated in the amino acid pathway together with the association differential metabolites of amino acid are tea-specific responses for COS treatment. In brief, COS could appreciably enhance the gene expression concerned with photosynthesis, carbon metabolism, nitrogen, amino acid metabolism, and metabolic response modification

in tea plants, especially secondary metabolism, hence promoting the growth of tea plants. These related genes are the potential targets of chitosan-mediated growth stimulation in various plants [44,47,48].

Altogether, in this study, the transcriptome and metabolome of tea leaves from the control and COS treatment were performed by association analyses. Information about the differential expressed genes and metabolites was obtained. Furthermore, the transcriptome datasets and analysis reported here will facilitate functional genomics, gene discovery, and transcriptional regulation of COS in tea plants. It provided a systemic insight into the mechanism of chitosan oligosaccharides on tea plant growth promotion and formed a theoretical basis for the application of chitosan oligosaccharides in tea plants.

4. Materials and Methods

4.1. Field Experiment, Sample Collection and Yield Estimate

Field tests were conducted at a tea garden in Meitan (Longitude: 107.48 latitude: 27.7) in Guizhou Province, China. The tested tea plants (*Camellia sinensis* var. *Sinensis*, Qianmei 601.) were around 10 years old and free of pesticide application during the test.

5% COS agents were purchased from Hainan Zhengye Zhongnong High-tech Co., Ltd., Haikou, China. The commercial agent was diluted with water 500, 800, and 1000 times in volume, and water consumption was 32 kg for one mu (667 m²). The actual dose of COS was 3.2, 2.0, and 1.6 g/667 m², respectively. The adjacent plot with no COS spraying served as a control (CK). There were three replicates in the randomized complete block for every spraying application in the tea garden. Seven days after spraying COS, yields in the control and COS-treated group were allowed to estimate in randomly selected tea plant rows in the center of the field. The number of buds in each of 0.1 m² (0.33 m × 0.33 m) was counted, and the mean bud density (buds per square meter) for each plot was calculated. The obtained tea buds were randomly selected, and the weight of the 100 tea buds was measured. All measurements were repeated three times. Finally, the tea buds picked in each treatment group were quickly frozen with liquid nitrogen and stored in a −80 °C freezer.

4.2. Determination of Chlorophyll, Soluble Sugar and Amino Acid Content

In the controls and COS-treated leaves, the content of chlorophyll soluble sugar and amino acids was measured and expressed as mg/g FW (fresh weight). Among them, chlorophyll and soluble sugar content were determined by following the provisions in bioassay kits, as previously reported [28]. The amino acid content was determined according to GB/T8314-2013 determination of total free amino acids in tea. The involved bioassay kits were purchased from Solarbio, Beijing, China.

4.3. Transcriptomic Profiling

RNA sequencing was used to analyze the transcriptome of samples from the control and COS treatment groups, treated at a concentration of 2.0 g/667 m² ($n = 3$ for both groups, six samples in total) as previous description [28]. The extraction of total RNAs was done by using TRIzol (Invitrogen, Carlsbad, CA, USA). The concentration of isolated RNA was determined by NanoDrop TM OneC spectrophotometer (Thermo Fisher Scientific Inc., Carlsbad, CA, USA). The quality and integrity of RNA were checked by running a 1.5% agarose gel. The cDNA synthesis was finished by using 2 ug DNase-treated RNA using a cDNA synthesis kit (Thermo Fisher Scientific Inc., Carlsbad, CA, USA). The mRNA libraries were generated using KC-DigitalTM stranded mRNA libraryprep kit for Illumina[®] (Catalog NO. DR08502, Seqhealth Technology Co., Ltd., Wuhan, China), and the library quality was assessed on the Agilent Bioanalyzer 2100 system. The kit eliminates duplication bias in PCR and sequencing steps by using a unique molecular identifier (UMI) of eight random bases to label the pre-amplified cDNA molecules. The library products corresponding to 200–500 bps were enriched, quantified, and finally sequenced on Illumina Novaseq 6000 (Illumina, San Diego, CA, USA). RNA extraction, library preparation, and data analysis of high-throughput sequencing were completed by Kangce Technology Co., Ltd.

in Wuhan, China. For RNA-Seq data analysis, raw sequencing data were first analyzed by FastQC, and low-quality reads were filtered by Trimmomatic (version 0.36) and discarded. The reads contaminated with adaptor sequences were trimmed, and then clean reads were mapped to the reference genome of *Camellia sinensis* using STATR software (version 2.5.3a). Estimation of gene expression level using Fragments Per Kilobase Million (FPKM) method. All assembled unigenes were annotated in the following databases: GO and KEGG. Differentially expressed genes (DEGs) between the two groups were identified using edgeR software (version 3.12.1). FDR-corrected $p < 0.05$ with a fold change ≥ 2 was used to determine whether the differential genes were statistically significant. Differential gene GO, and KEGG data analysis was performed using KOBAS software (version 2.1.1) with a corrected $p < 0.05$ to determine if the enrichment was statistically significant. To infer the putative functions of DEGs, we conducted GO enrichment analysis using top GO and KEGG pathways and enrichment analysis using cluster Profiler (version R 3.6.0, October 2019).

4.4. Metabolite Profiling

4.4.1. Extraction and Detection of Metabolites

Tea leaves (100 mg) from the COS treatment (HAI7_2) and control (KB7_1) were ground with liquid nitrogen, and the homogenate was resuspended with prechilled 80% methanol and 0.1% formic acid using a vortex. The samples were incubated on ice for 5 min and then centrifuged at $15,000 \times g$, 4°C for 20 min. Some supernatants were diluted to a final concentration containing 53% methanol with LC-MS-grade water. The samples were subsequently transferred to a fresh Eppendorf tube and were then centrifuged at $15,000 \times g$, 4°C for 20 min. Finally, the supernatant was injected into the LC-MS/MS system analysis [49]. UHPLC-MS/MS analyses were performed using a Vanquish UHPLC system (Thermo Fisher Scientific GmbH, Dreieich, Germany) coupled with an Orbitrap Q ExactiveTM HF-X mass spectrometer (Thermo Fisher, Dreieich, Germany) by Novogene Co., Ltd. in Beijing, China. The raw data files generated by UHPLC-MS/MS were processed using Compound Discoverer 3.1 (Thermo Fisher, Dreieich, Germany) to perform peak alignment, peak picking, and quantitation for each metabolite. Peaks were then matched with the mzCloud (<https://www.mzcloud.org/>, accessed on 26 October 2020), mzVault, and MassList databases to obtain accurate qualitative and relative quantitative results. Statistical analyses were performed using the statistical software R (R version R-3.4.3), Python (Python 2.7.6 version), and CentOS (CentOS release 6.6); when data were not normally distributed, normal transformations were attempted using of area normalization method. The metabolomic sampling method is the same as the transcriptome analysis experiment, and three biological replicates are set for each treatment.

4.4.2. Data Processing and Statistics

These metabolites were annotated using the KEGG database (<https://www.genome.jp/kegg/pathway.html>, accessed on 26 October 2020), HMDB database (<https://hmdb.ca/metabolites>, accessed on 26 October 2020), and LIPI Maps database (<http://www.lipidmaps.org/>, accessed on 26 October 2020). Principal components analysis (PCA) was performed at meta-X (a flexible and comprehensive software for processing metabolomics data). We applied univariate analysis (t -test) to calculate the statistical significance (p -value). The metabolites with $\text{VIP} > 1$ and p -value < 0.05 and fold change (FC) ≥ 2 or $\text{FC} \leq 0.5$ were considered to be differential metabolites.

For clustering heat maps, the data were normalized using z-scores of the intensity areas of differential metabolites and were plotted by pheatmap package in R language. The correlation between differential metabolites was analyzed by "cor ()" in R language (method = "Pearson"). Statistically significant correlation between differential metabolites was calculated by "cor.test ()" in R language. A p -value < 0.05 was considered statistically significant, and correlation plots were plotted by corrplot package in R language. The functions of these metabolites and metabolic pathways were studied using the KEGG database.

4.5. Validation of qRT-PCR

To verify the reliability of transcriptome sequencing results, we selected seven DEGs associated with tea plant defense for qRT-PCR analysis. Gene-specific primers (Table S13) were designed. Additionally, qRT-PCR was performed on a Light Cycler 96 System in a 20 mL reaction volume under the following parameters: 95 °C for 15 s, 60 °C for 30 s, and 72 °C for 30 s for 40 cycles. GAPDH was used as a reference gene, and relative gene expression was calculated using the $2^{-\Delta\Delta C_t}$ method [50].

4.6. Statistical Analysis

Data were expressed as the mean \pm standard error, and the data were subjected to a one-way analysis of variance (ANOVA A) ($p < 0.05$) followed by a significant difference test (LSD) using SPSS statistics v16.0 (SPSS Inc., Chicago, IL, USA).

Supplementary Materials: The following supporting information can be downloaded at: <https://www.mdpi.com/article/10.3390/ijms23105469/s1>.

Author Contributions: D.J. conducted the experiments; D.J., L.O. and L.J. designed and performed the experiments; D.J., X.R., X.Y. and Y.T. took part in the field test and analyzed the data; L.J. conceived and supervised the project; X.Z. wrote the manuscript. All authors have read and agreed to the published version of the manuscript.

Funding: This research was funded by Guizhou province's science and technology project, (2015)5020, and scientific research projects of major agricultural industries of Guizhou province, (2019)006.

Institutional Review Board Statement: Not applicable.

Informed Consent Statement: Not applicable.

Data Availability Statement: All data in the manuscript are available from the corresponding author upon request.

Conflicts of Interest: The authors declare no conflict of interest.

References

1. Wu, Z.J.; Ma, H.Y.; Zhuang, J. ITRAQ-based proteomics monitors the withering dynamics in postharvest leaves of tea plant (*Camellia sinensis*). *Mol. Genet. Genom.* **2017**, *293*, 45–59. [CrossRef] [PubMed]
2. Jayasinghe, S.L.; Kumar, L. Potential impact of the current and future climate on the yield, quality, and climate suitability for tea [*Camellia sinensis* (L.) O. Kuntze]: A systematic review. *Agronomy* **2021**, *11*, 619. [CrossRef]
3. Kumar, A.; Seema. Monitoring of fluoride contamination and correlation with physicochemical parameters of surface soil and ground water near tea-garden of Thakurganj block of Kishanganj, Bihar, India. *Am. J. Environ. Eng.* **2016**, *6*, 38–51.
4. Zhou, Y. Risk regulation in the application of the pesticide residue standards—A case study of Chinese tea. *Sch. J. Agric. Vet. Sci.* **2016**, *3*, 389–394.
5. Mourato, S.; Ozdemiroglu, E.; Foster, V. Evaluating health and environmental impacts of pesticide use: Implications for the design of ecolabels and pesticide taxes. *Environ. Sci. Technol.* **2000**, *34*, 1456–1461. [CrossRef]
6. Chen, H.; Hao, Z.X.; Wang, Q.H.; Jiang, Y.; Pan, R.; Wang, C.; Liu, X.; Lu, C.Y. Occurrence and risk assessment of organophosphorus pesticide residues in Chinese tea. *Hum. Ecol. Risk Assess. Int. J.* **2016**, *22*, 28–38. [CrossRef]
7. Minhas, P.S.; Rane, J.; Pasala, R.K. Plant Bioregulators: A Stress Mitigation Strategy for Resilient Agriculture. In *Abiotic Stress Management for Resilient Agriculture*; Minhas, P., Rane, J., Pasala, R., Eds.; Springer: Singapore, 2017; pp. 235–259.
8. Mukarram, M.; Khan, M.; Choudhary, S.; Zehra, A.; Aftab, T. Natural Polysaccharides: Novel Plant Growth Regulators. In *Plant Growth Regulators*; Aftab, T., Hakeem, K.R., Eds.; Springer: Aligarh, India, 2021; pp. 335–354.
9. Mzibra, A.; Aasfar, A.; El Arroussi, H.; Khouloud, M.; Dhiba, D.; Kadmiri, I.M.; Bamouh, A. Polysaccharides extracted from moroccan seaweed: A promising source of tomato plant growth promoters. *J. Appl. Phycol.* **2018**, *30*, 2953–2962. [CrossRef]
10. Mondal, M.; Malek, M.A.; Puteh, A.B.; Ismail, M.R.; Naher, L. Effect of foliar application of chitosan on growth and yield inokra. *Aust. J. Crop Sci.* **2012**, *6*, 918–921.
11. Xia, W.; Liu, P.; Zhang, J.; Chen, J. Biological activities of chitosan and chitoooligosaccharides. *Food Hydrocoll.* **2011**, *25*, 170–179. [CrossRef]
12. Badawy, M.; Rabea, E.I. A biopolymer chitosan and its derivatives as promising antimicrobial agents against plant pathogens and their applications in crop protection. *Int. J. Carbohydr. Chem.* **2011**, *2011*, 29. [CrossRef]

13. Manjunatha, G.; Roopa, K.S.; Prashanth, G.N.; Shekar Shetty, H. Chitosan enhances disease resistance in pearl millet against downy mildew caused by *Sclero-spora graminicola* and defence-related enzyme activation. *Pest Manag. Sci. Former. Pestic. Sci.* **2008**, *64*, 1250–1257. [[CrossRef](#)] [[PubMed](#)]
14. Katiyar, D.; Hemantaranjan, A.; Singh, B.; Bhanu, A.N. A future perspective in crop protection: Chitosan and its oligosaccharides. *Adv. Plants Agric. Res.* **2014**, *1*, 6.
15. Wink, M. Plant breeding: Importance of plant secondary metabolites for protection against pathogens and herbivores. *Theor. Appl. Genet.* **1988**, *75*, 225–233. [[CrossRef](#)]
16. Chibu, H.; Shibayama, H.; Arima, S. Effects of chitosan application on the shoot growth of rice and soybean. *Jpn. J. Crop Sci.* **2002**, *71*, 212–219. [[CrossRef](#)]
17. Rabea, E.I.; Badawy, M.E.; Steurbaut, W.; Stevens, C.V. In vitro assessment of N-(benzyl) chitosan derivatives against some plant pathogenic bacteria and fungi. *Eur. Polym. J.* **2009**, *45*, 237–245. [[CrossRef](#)]
18. Sathiyabama, M.; Akila, G.; Charles, R.E. Chitosan-induced defence responses in tomato plants against early blight disease caused by *Alternaria solani* (Ellis and Martin) Sorauer. *Arch. Pflanzenschutz* **2014**, *47*, 1963–1973. [[CrossRef](#)]
19. Islam, M.M.; Kabir, M.H.; Mamun, A.; Islam, M.; Das, P. Studies on yield and yield attributes in tomato and chilli using foliar application of oligo-chitosan. *GSC Biol. Pharm. Sci.* **2018**, *3*, 20–28. [[CrossRef](#)]
20. Ibraheim, S.; Mohsen, A. Effect of chitosan and nitrogen rates on growth and productivity of summer squash plants. *Middle East* **2015**, *4*, 673–681.
21. Sheikha, S.; Al-Malki, F.M. Growth and chlorophyll responses of bean plants to the chitosan applications. *Eur. J. Sci. Res.* **2011**, *50*, 124–134.
22. Falcón-Rodríguez, A.B.; Costales, D.; González-Pea, D.; Morales, D.; Cabrera, J.C. Chitosans of different molecular weight enhance potato (*Solanum tuberosum* L.) yield in a field trial. *Span. J. Agric. Res.* **2017**, *15*, e0902. [[CrossRef](#)]
23. Wang, M.; Chen, Y.; Zhang, R.; Wang, W.; Zhao, X.; Du, Y.; Yin, H. Effects of chitosan oligosaccharides on the yield components and production quality of different wheat cultivars (*Triticum aestivum* L.) in Northwest China. *Field Crops Res.* **2015**, *172*, 11–20. [[CrossRef](#)]
24. Tham, L.X.; Nagasawa, N.; Matsushashi, S.; Kume, T. Effect of radiation-degraded chitosan on plants stressed with vanadium. *Radiat. Phys. Chem.* **2001**, *61*, 171–175. [[CrossRef](#)]
25. Yan, L.; Wei, L.J.; Wang, Q.; Li, H.; Zhao, X.; Hou, H.; Du, Y. Effects of oligochitosan on photosynthetic parameter of *Brassica napus* L. leaves. *Chin. Agric. Sci. Bull.* **2010**, *26*, 132–136.
26. Zhang, X.; Li, K.; Xing, R.; Liu, S.; Li, P. Metabolite profiling of wheat seedlings induced by chitosan: Revelation of the enhanced carbon and nitrogen metabolism. *Front. Plant Sci.* **2017**, *8*, 2017. [[CrossRef](#)] [[PubMed](#)]
27. Ou, L.; Zhang, Q.; Ji, D.; Li, Y.; Zhou, X.; Jin, L. Physiological, transcriptomic investigation on the tea plant growth and yield motivation by chitosan oligosaccharides. *Horticulturae* **2022**, *8*, 68. [[CrossRef](#)]
28. Li, Y.; Zhang, Q.; Ou, L.; Ji, D.; Liu, T.; Lan, R.; Li, X.; Jin, L. Response to the cold stress signaling of the tea plant (*Camellia sinensis*) elicited by chitosan oligosaccharide. *Agronomy* **2020**, *10*, 915. [[CrossRef](#)]
29. Zhao, Q.; Zhang, H.; Wang, T.; Chen, S.; Dai, S. Proteomics-based investigation of salt-responsive mechanisms in plant roots. *J. Proteom.* **2013**, *82*, 230–253. [[CrossRef](#)]
30. Zhou, Y.; Zhang, L.; Zeng, K. Efficacy of *Pichia membranaefaciens* combined with chitosan against *Colletotrichum gloeosporioides* in citrus fruits and possible modes of action. *Biol. Control* **2016**, *96*, 39–47. [[CrossRef](#)]
31. Winkler, A.J.; Dominguez-Nunez, J.A.; Aranaz, I.; Poza-Carrion, C.; Ramonell, K.; Somerville, S.; Berrocal-Lobo, M. Short-chain chitin oligomers: Promoters of plant growth. *Mar. Drugs* **2017**, *15*, 40. [[CrossRef](#)]
32. Wang, H.; Guo, X.; Li, Q.; Lu, Y.; Yan, S. Integrated transcriptomic and metabolic framework for carbon metabolism and plant hormones regulation in *Vigna radiata* during post-germination seedling growth. *Sci. Rep.* **2020**, *10*, 3745. [[CrossRef](#)]
33. An, L.; Ma, J.; Wang, H.; Li, F.; Qin, D.; Wu, J.; Zhu, G.; Zhang, J.; Yuan, Y.; Zhou, L.; et al. NMR-based global metabolomics approach to decipher the metabolic effects of three plant growth regulators on strawberry maturation. *Food Chem.* **2018**, *269*, 559–566. [[CrossRef](#)] [[PubMed](#)]
34. Pang, X.; Suo, J.; Liu, S.; Xu, J.; Yang, T.; Xiang, N.; Wu, Y.; Lu, B.; Qin, R.; Liu, H.; et al. Combined transcriptomic and metabolomic analysis reveals the potential mechanism of seed germination and young seedling growth in *Tamarix hispida*. *BMC Genom.* **2022**, *23*, 109. [[CrossRef](#)] [[PubMed](#)]
35. Dzung, N.A.; Khanh, V.; Dzung, T.T. Research on impact of chitosan oligomers on biophysical characteristics, growth, development and drought resistance of coffee. *Carbohydr. Polym.* **2011**, *84*, 751–755. [[CrossRef](#)]
36. Dalio, R.; Pinheiro, H.P.; Sodek, L.; Haddad, C. The effect of 24-epibrassinolide and clotrimazole on the adaptation of *Cajanus cajan* (L.) Millsp. to salinity. *Acta Physiol. Plant.* **2011**, *33*, 1887–1896. [[CrossRef](#)]
37. Balal, R.M.; Shahid, M.A.; Javaid, M.M.; Iqbal, Z.; Liu, G.D.; Zotarelli, L.; Khan, N. Chitosan alleviates phytotoxicity caused by boron through augmented polyamine metabolism and antioxidant activities and reduced boron concentration in *Cucumis sativus* L. *Acta Physiol. Plant.* **2017**, *39*, 31. [[CrossRef](#)]
38. Dar, T.A.; Uddin, M.; Khan, M.M.A.; Ali, A.; Mir, S.R.; Varshney, L. Effect of Co-60 gamma irradiated chitosan and phosphorus fertilizer on growth, yield and trigonelline content of *Trigonella foenum-graecum* L. *J. Radiat. Res. Appl. Sci.* **2015**, *8*, 446–458. [[CrossRef](#)]

39. Uthairatanakij, A.; Silva, J.; Obsuwan, K. Chitosan for improving orchid production and quality. *Orchid. Sci. Biotechnol.* **2007**, *1*, 1–5.
40. Ahmed, A.; Nesiem, A.E.; Allam, H.A.; El-Wakil, A.F. Effect of pre-harvest chitosan foliar application on growth, yield and chemical composition of Washington navel orange trees grown in two different regions. *Afr. J. Biochem. Res.* **2016**, *10*, 59–69. [[CrossRef](#)]
41. Studer, A.J.; Gandin, A.; Kolbe, A.R.; Wang, L.; Cousins, A.B.; Brutnell, T.P. A limited role for carbonic anhydrase in C4 photosynthesis as revealed by a ca1ca2 double mutant in maize. *Plant Physiol.* **2014**, *165*, 608. [[CrossRef](#)]
42. Rueda-López, M.; Cañas, R.A.; Canales, J.; Cánovas, F.M.; Ávila, C. The overexpression of the pine transcription factor PpDof5 in Arabidopsis leads to increased lignin content and affects carbon and nitrogen metabolism. *Physiol. Plant.* **2015**, *155*, 369–383. [[CrossRef](#)]
43. Masahiro, T.; Miki, N.; Yukinori, Y.; Shigeru, S. Carbon metabolism in the Calvin cycle. *Plant Tissue Cult. Lett.* **2005**, *22*, 355–360.
44. Zhang, X.; Li, K.; Xing, R.; Liu, S.; Chen, X.; Yang, H.; Li, P. miRNA and mRNA expression profiles reveal insight into chitosan-mediated regulation of plant growth. *J. Agric. Food Chem.* **2018**, *66*, 3810–3822. [[CrossRef](#)] [[PubMed](#)]
45. Akimoto-Tomiyama, C.; Sakata, K.; Yazaki, J.; Nakamura, K.; Fujii, F.; Shimbo, K.; Yamamoto, K.; Sasaki, T.; Kishimoto, N.; Kikuchi, S. Rice gene expression in response to *N*-acetylchitoooligosaccharide elicitor: Comprehensive analysis by DNA microarray with randomly selected ESTs. *Plant Mol. Biol.* **2003**, *52*, 537–551. [[CrossRef](#)] [[PubMed](#)]
46. Fontaine, J.X.; Terce-Laforgue, T.; Armengaud, P.; Clement, G.; Renou, J.P.; Pelletier, S.; Catterou, M.; Azzopardi, M.; Gibon, Y.; Lea, P.J. Characterization of a NADH-dependent glutamate dehydrogenase mutant of arabidopsis demonstrates the key role of this enzyme in root carbon and nitrogen metabolism. *Plant Cell* **2012**, *24*, 4044–4065. [[CrossRef](#)] [[PubMed](#)]
47. Elboutachfaiti, R.; Molinié, R.; Mathiron, D.; Maillot, Y.; Fontaine, J.X.; Pilard, S.; Quéro, A.; Brasselet, C.; Dols-Lafargue, M.; Delattre, C.; et al. Secondary metabolism rearrangements in *Linum usitatissimum* L. after biostimulation of roots with COS oligosaccharides from fungal cell wall. *Molecules* **2022**, *27*, 2372. [[CrossRef](#)]
48. Chamnanmanoontham, N.; Pongprayoon, W.; Pichayangkura, R.; Roytrakul, S.; Chadchawan, S. Chitosan enhances rice seedling growth via gene expression network between nucleus and chloroplast. *Plant Growth Regul.* **2015**, *75*, 101–114. [[CrossRef](#)]
49. Want, E.J.; Masson, P.; Michopoulos, F.; Wilson, I.D.; Theodoridis, G.; Plumb, R.S.; Shockcor, J.; Loftus, N.; Holmes, E.; Nicholson, J.K. Global metabolic profiling of animal and human tissues via UPLC-MS. *Nat. Protoc.* **2013**, *8*, 17–32. [[CrossRef](#)]
50. Livak, K.J.; Schmittgen, T.D. Analysis of relative gene expression data using real-time quantitative PCR and the 2(-Delta Delta C(T)) method. *Methods* **2013**, *25*, 402–408. [[CrossRef](#)]